

# CP-LLM: Context and Pixel Aware Large Language Model for Video Quality Assessment

Wen Wen<sup>1\*</sup> Yaohong Wu<sup>2</sup> Yue Sheng<sup>2</sup> Neil Birkbeck<sup>2</sup>  
 Balu Adsumilli<sup>2</sup> Yilin Wang<sup>2†</sup>

<sup>1</sup>City University of Hong Kong <sup>2</sup>Google Inc.  
 wwen29-c@my.cityu.edu.hk

{yaohongwu, yueshengys, birkbeck, badsumilli, yilin}@google.com

## Abstract

Video quality assessment (VQA) is a challenging research topic with broad applications. Effective VQA necessitates sensitivity to pixel-level distortions and a comprehensive understanding of video context to accurately determine the perceptual impact of distortions. Traditional hand-crafted and learning-based VQA models mainly focus on pixel-level distortions and lack contextual understanding, while recent LLM-based models struggle with sensitivity to small distortions or handle quality scoring and description as separate tasks. To address these shortcomings, we introduce **CP-LLM**: a Context and Pixel aware Large Language Model. CP-LLM is a novel multimodal LLM architecture featuring dual vision encoders designed to independently analyze perceptual quality at both high-level (video context) and low-level (pixel distortion) granularity, along with a language decoder subsequently reasons about the interplay between these aspects. This design enables CP-LLM to simultaneously produce robust quality scores and interpretable quality descriptions, with enhanced sensitivity to pixel distortions (*e.g.* compression artifacts). The model is trained via a multi-task pipeline optimizing for score prediction, description generation, and pairwise comparisons. Experiment results demonstrate that CP-LLM achieves state-of-the-art cross-dataset performance on established VQA benchmarks and superior robustness to pixel distortions, confirming its efficacy for comprehensive and practical video quality assessment in real-world scenarios.

## 1 Introduction

Video quality assessment (VQA) is a fundamental research area with broad applications in video compression, transcoding, transmission, playback, content search, and recommendation systems. While subjective testing by human raters remains the most reliable method for quality evaluation, its inherent expense, time-consuming nature, and scalability limitations preclude its application at large scale. Consequently, the development of accurate and robust objective VQA models has been a central focus of research over the past decades. Objective VQA models can be broadly categorized based on the availability of a reference video: no-reference models assess a single target video, whereas full-reference models compare the target video against a pristine reference [22, 11, 37]. However, full-reference models operate under the assumption that the reference video is of superior quality, an assumption that falters when dealing with non-pristine or enhanced original content, thereby limiting their reliability. Conversely, certain no-reference models [20] have demonstrated considerable potential in applications traditionally dominated by full-reference approaches, such

\*Work done during internship at Google

†Corresponding authors.

							
Human	Good	Human	Good	Human	Good	Human	Good
Gemini 2.0	Good	Gemini 2.0	Good	Gemini 2.0	Good	Gemini 2.0	Good
CoINVQ	2.5 (Fair)	CoINVQ	2.9 (Fair)	CoINVQ	2.9 (Fair)	CoINVQ	2.9 (Fair)
FastVQA	1.6 (Bad)	FastVQA	3.7 (Fair)	FastVQA	3.2 (Fair)	FastVQA	1.5 (Bad)
DOVER	1.6 (Bad)	DOVER	3.6 (Fair)	DOVER	3.1 (Fair)	DOVER	1.4 (Bad)

Figure 1: Videos with intentional effects but incorrectly identified as quality defects by traditional VQA models (CoINVQ [20], FastVQA [25], and DOVER [26]), while MLLM’s assessment aligns better with human perception. The first two videos contain intentional low-light and background blurring. The third video presents an astronomy video containing complex visual textures. The last video shows a pixel-art style game characterized by inherent blockiness. All quality scores are calibrated to [1, 5], where 1, 2, 3, 4, 5 correspond to bad, poor, fair, good, and excellent respectively.





			
Prompt	Which image has better perceptual quality: the first or the second?		
<b>Ground truth</b>	<b>First.</b>		
Human	First.	✓	
CoINVQ	First: 4.332	Second: 4.301	✓
GPT-4o	I cannot directly compare the perceptual quality of the two images.		
Gemini 2.0	Both images are identical. Therefore, the perceptual quality is the same.		

Figure 2: An original video (left) and its compressed version (right). The quality degradation is easily detected by human and VQA models (*e.g.* CoINVQ), but not correctly caught by MLLMs.

as video compression assessment, while offering greater flexibility for evaluating enhanced videos. Given these considerations, this paper primarily focuses on the advancement of no-reference VQA.

Early no-reference VQA models predominantly concentrated on quantifying low-level signal distortions, such as blur, noise, and blocking artifacts [13, 12, 7, 17, 8]. However, with the emergence of user-generated content (UGC) videos, several subjective studies [19, 21] have demonstrated that identical low-level artifacts can elicit significantly different perceptual quality ratings. Consequently, effective UGC-VQA necessitates a comprehensive analysis encompassing both low-level pixel distortions and high-level semantic information. Recognizing this imperative, an increasing number of recent methodologies have aimed to explicitly integrate high-level semantic insights into their model architectures. For instance, Wang *et al.* [20] developed a learning-based model employing three specialized subnetworks to independently address content, distortion, and compression aspects. These subnetworks subsequently feed their extracted representations into an aggregation network for final score regression. Adopting a similar strategy, Tu *et al.* [18] combined traditional hand-crafted low-level signals with features derived from a convolutional neural network (CNN) to capture high-level semantics, thereby enhancing quality prediction.

Although approaches mentioned above underscored the value of leveraging semantic signals, they possess limitations, notably in their content understanding capabilities. As illustrated in Figure 1, certain visual artifacts (*e.g.*, dark scenes, intentional blur, pixelation) that are integral to the artistic style or narrative of the content are often misinterpreted as quality defects by state-of-the-art (SOTA) VQA models such as CoINVQ [20], FastVQA [25], and DOVER [26]. In contrast, advanced multimodal large language models (MLLMs) like Gemini and GPT have demonstrated the capacity

to correctly interpret these stylistic choices as intended, thereby rating such examples as high quality and highlighting a crucial capability absent in many current VQA models.

The emergence of MLLMs offers a promising new paradigm for VQA, as explored in recent studies [31, 27, 38]. However, current MLLM applications in VQA encounter several critical challenges. Many implementations rely on pre-existing MLLMs whose vision encoders are primarily optimized for high-level semantic understanding rather than detailed perceptual analysis. While this semantic orientation is advantageous for interpreting diverse content (as exemplified in Figure 1), it can impede nuanced quality assessment, particularly in discerning pixel-level distortions (see Figure 2). Furthermore, the vision encoders in MLLMs typically operate on fixed, low-resolution inputs, necessitating input image resizing that frequently disregards the original aspect ratio and can consequently introduce additional localized distortions. Although some recent work [35] utilized a full-reference paradigm to compare images from the same source with varying artifacts, the assessment of distortion levels still remain coarse, failing to guarantee sensitivity to pixel distortions that impact perceived video quality. Additionally, a majority of existing works utilize MLLMs either exclusively for generating quality-related descriptions [28, 30, 35, 34] or solely for predicting quality scores [29, 33, 24, 4].

To address these prevailing limitations, we introduce CP-LLM, a novel MLLM-based VQA framework explicitly designed to detect pixel-level artifacts while simultaneously providing robust score predictions and pertinent content- and quality-related descriptions. The work delivers the following key contributions:

- An MLLM-based VQA model capable of simultaneously generating quality score predictions and interpretable perceptual descriptions.
- A novel framework ensuring the model excels concurrently at single-video quality prediction, pairwise quality comparisons, and the generation of coherent quality descriptions.
- A comprehensive experiment design that evaluates both accuracy and robustness of VQA model, with novel evaluation criteria (*e.g.* flip rate) that have not been sufficiently addressed in existing VQA evaluations.

## 2 Related Work

**Knowledge-driven and Learning-based Methods.** Objective methods for assessing UGC video quality have evolved significantly in past decades. Early knowledge-driven approaches, such as V-BLIINDS [13], VIIDEO [12], TLVQM [7], and VIDEVAL [17], primarily relied on handcrafted spatial and temporal features. Subsequently, hybrid models like CNN-TLVQM [8] and RAPIQUE [18] combined these handcrafted features with representations learned by pretrained CNNs. More recently, purely learning-based models become more and more popular. One common strategy is to employ pretrained networks as separate feature extractors and aggregate features by a subsequent regression module, where relevant works includes VSFA [10], Li22 [9], PVQ [32], and CoINVQ [20]. Another direction focuses on end-to-end fine-tuning of the entire network, as demonstrated in SimpleVQA [14] and MinimalisticVQA [15]. Further advancements include specialized end-to-end techniques, such as the fragment-based processing in FastVQA [25], the incorporation of aesthetic features in DOVER [26], and the use of modular designs targeting specific quality factors like content, resolution, and frame rate in MBVQA [23].

**MLLM-based Methods.** Different from traditional VQA models, MLLM-based methods leverage the extensive knowledge embedded within MLLMs to provide detailed descriptions related to video content and enhance the interpretability of quality assessment. One branch of this research focuses primarily on improving the descriptive capabilities of MLLMs for VQA tasks. For instance, Q-Instruct [28], Co-Instruct [30], DepictQA [35], and DepictQA-Wild [34] employ specialized datasets and tailored fine-tuning strategies to enhance the low-level perceptual abilities required for nuanced quality descriptions. Conversely, other approaches prioritize direct quality score prediction. Models like Q-Align [29] and DeQA-Score [33] harness the perceptual understanding of MLLMs specifically to generate accurate scores. Similarly, LLM-VQA [4] incorporated SlowFast [3] motion features to improve the capture of temporal distortions, aiming for more accurate score prediction.

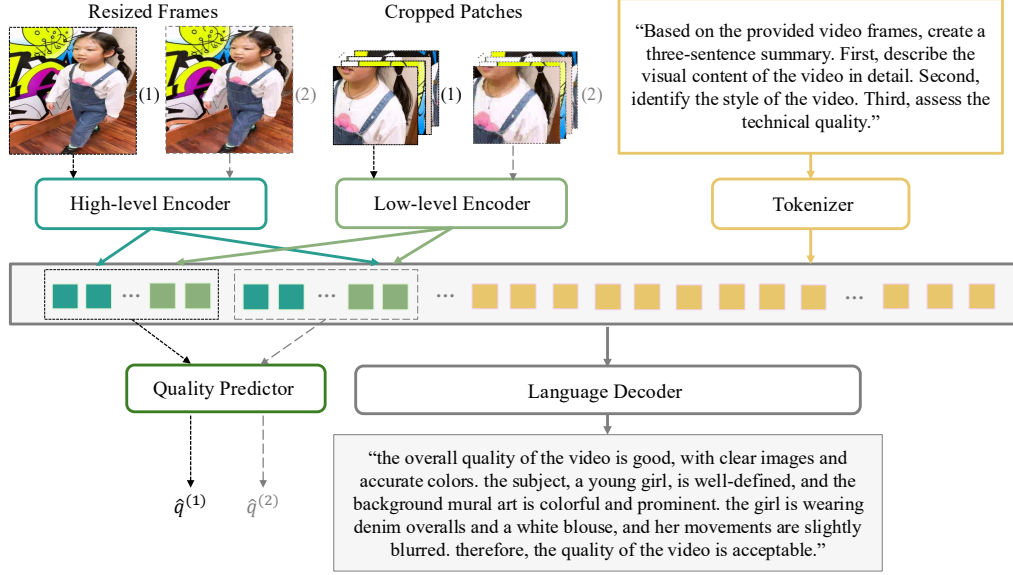


Figure 3: The overview of CP-LLM framework. The model processes video frames through two distinct visual pathways: a high-level encoder extracts semantic features, and a low-level encoder captures fine-grained perceptual details from image patches. Embeddings from both visual streams are interleaved with text prompt embeddings and fed into a language decoder to generate textual output. Concurrently, both the concatenated visual embeddings are processed by an MLP regression head to predict a numerical quality score.

### 3 CP-LLM: Context and Pixel aware Large Language Model

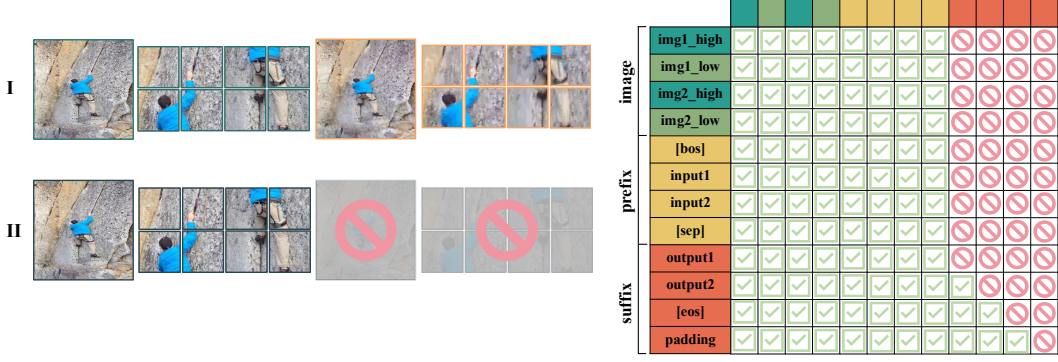
#### 3.1 Model Components

To achieve good context understanding capability and good sensitivity to pixel distortions, the proposed CP-LLM model incorporates an MLLM architecture with dual vision encoders: one encoder is dedicated to extracting high-level semantic information, while the other focuses on capturing low-level, fine-grained texture details. Features derived from both vision encoders are processed by a quality predictor to get an overall quality score. Meanwhile, these features are concatenated with prompt embeddings and fed into a language decoder to generate comprehensive quality descriptions. The overall structure of CP-LLM is depicted in Figure 3, and the details of four major components are discussed in the following subsections.

##### 3.1.1 High-level Encoder

The high-level vision encoder extracts semantic information and supports downsampling input frames to a lower resolution, ensuring a comprehensive understanding of the overall video context.

We denote a video sequence as  $\mathbf{x} = \{\mathbf{x}_i\}_{i=0}^{N-1}$ , where  $\mathbf{x}_i \in \mathbb{R}^{H \times W \times 3}$  represents the  $i$ -th frame,  $H$  and  $W$  are the original frame height and width, and  $N$  is the total number of frames in the sequence. We first uniformly sample a sparse set of  $M$  key frames, denoted as  $\mathbf{y} = \{\mathbf{y}_i\}_{i=0}^{M-1}$ , from the original sequence  $\mathbf{x}$ . Each selected key frame  $\mathbf{y}_i \in \mathbb{R}^{H \times W \times 3}$  undergoes preprocessing. A vision encoder  $\mathbf{f}_h(\cdot)$  processes the input frame  $\mathbf{y}_i$  after bilinear resizing to  $H_h \times W_h$ . This encoder outputs a sequence of contextualized visual embeddings  $\mathbf{u}_i = \mathbf{f}_h(\mathbf{y}_i)$ .  $\mathbf{u}_i$  is then projected through a linear layer to align with a target dimension  $D$  (specifically, the embedding dimension of language decoder), resulting  $\mathbf{u}_i \in \mathbb{R}^{T_h \times D}$ .



(a) The input pipeline of CP-LLM requires two inputs (case I), and a single input frame (case II) will be duplicated to serve as padding and then masked out from the decoder. (b) Visualization of the attention mask for CP-LLM, configured with a prefix language model attention strategy.

Figure 4: The input pipeline and corresponding attention mask of CP-LLM.

### 3.1.2 Low-level Encoder

Targeting fine-grained pixel distortions, the low-level vision encoder operates on input frames at a significantly higher resolution and accurately preserves their aspect ratio to prevent introducing unexpected distortions.

The frame  $y_i$  is resized using bilinear interpolation to a fixed resolution  $H_l \times W_l$ . Subsequently, we extract  $K$  non-overlapping patches,  $\mathcal{P}_i = \{p_{i,j}\}_{j=0}^{K-1}$ , uniformly from the resized frame, where each patch  $p_{i,j} \in \mathbb{R}^{H_p \times W_p \times 3}$  has a size  $H_p \times W_p$ . These  $K$  patches for each key frame  $y_i$  are then fed into a vision Transformer (ViT) model [2], denoted as  $f_l(\cdot)$ .  $f_l$  processes the patch sequence  $\mathcal{P}_i$  and outputs a corresponding sequence of feature embeddings  $h_i = \{h_{i,j}\}_{j=0}^{K-1}$ , where  $h_{i,j} \in \mathbb{R}^{T_q \times D_q}$ ,  $T_q$  is the number of tokens and  $D_q$  is the feature dimension of  $f_l$ . The features  $h_{i,j}$  are then projected through a linear layer to align with a target dimension  $D$  as well. To obtain a fixed-size representation for the frame while reducing the sequence length, we apply average pooling across the patch dimension and followed by a layer normalization, resulting in the final low-level embeddings  $v_i \in \mathbb{R}^{T_l \times D}$ .

### 3.1.3 Language Decoder

Language decoder is a critical component of the proposed CP-LLM. Unlike most existing VQA models [20, 26] that rely on a lightweight regressor to fuse high-level and low-level features, a powerful language decoder makes it possible to comprehensively consider all potential interactions between context and pixel distortions, and generate quality descriptions aligned with human reasoning.

To formalize the language decoder process, we denote the input as a pair  $(y_i, t_i)$ , where  $t_i$  represents the  $i$ -th input text prompt, typically provided as a sequence of tokens  $t_i = \{t_{i,j}\}_{j=0}^{L-1}$ , where  $L$  is the maximum length of the sequence. The proposed quality-aware vision-language model, which we can represent as a function  $g(\cdot, \cdot)$ , takes the image  $y_i$  and the text  $t_i$  as input, and generates an output text sequence  $z_i = \{z_{i,j}\}_{j=0}^{O-1}$ , where  $O$  is the maximum length of the generated output.

The visual embeddings derived from the input frame  $y_i$  consist of high level semantic features  $u_i$  and low level perceptual features  $v_i$ . Concurrently, the input text prompt tokens  $t_i$  are transformed into text embeddings  $r_i \in \mathbb{R}^{L \times D}$  by the language model's native embedding layer  $f_t(\cdot)$ . The language model decoder  $g$ , then receives an interleaved sequence formed by combining these three sets of features. Specifically, the input sequence for the decoder is constructed by concatenating the two visual embeddings and the embedded text prompt tokens:  $[u_i, v_i, r_i]$ . The decoder operates autoregressively to generate the output token sequence  $z_i$ . Each output token  $z_{i,k}$  is predicted based on the comprehensive context provided by the high level embeddings  $u_i$ , the low level visual features  $v_i$ , and all preceding tokens, which include the input prompt tokens  $t_i$  and previously generated output tokens  $\{z_{i,j}\}_{j=0}^{k-1}$ . This process is guided by a Prefix-LM attention mechanism, as visualized in Fig-

ure 4b. This generative process models the conditional probability  $p(z_{i,k} | \mathbf{u}_i, \mathbf{v}_i, \mathbf{t}_i, z_{i,0}, \dots, z_{i,k-1})$ , as determined by the decoder  $g$ .

### 3.1.4 Quality Predictor

To get an overall quality score is a basic requirement for VQA models. However, some recent studies [31] showed that MLLM is not good at directly rating video quality. Also from an efficiency perspective, reasoning through the entire language decoder just for a single quality score sounds a little over-killed. Thus in our CP-LLM framework, we introduce a light weight quality predictor to assess overall quality.

Our video quality predictor, denoted by the function  $f(\cdot) : \mathbb{R}^{(T_h+T_l) \times D} \mapsto \mathbb{R}$ , takes the concatenation of  $\mathbf{u}_i$  and  $\mathbf{v}_i$  as input and outputs a scalar quality score  $q_i$ . The quality predictor is a regression head, implemented as a two-layer multilayer perceptron (MLP) with a ReLU activation function between the fully connected layers, takes the visual embeddings as input and predicts a per-frame quality score. The overall quality score  $q$  for the video sequence  $\mathbf{x}$  is computed as the mean of the quality scores obtained from the  $M$  key frames.

## 3.2 Robust Multi-task Training Pipeline

The proposed CP-LLM model employs a multi-task training pipeline designed to integrate learning from diverse supervisory signals, accepting pairs of video variants as input, as shown in Figure 4a. This pipeline concurrently optimizes model parameters based on three core objectives central to comprehensive quality assessment:

First, a pairwise quality ranking loss,  $\mathcal{L}_1$ , encourages the model to correctly order the perceived quality between video variants within a pair:

$$\mathcal{L}_1 = \frac{1}{B} \sum_{i=1}^B \max(0, -(q_i^{(1)} - q_i^{(2)})(\hat{q}_i^{(1)} - \hat{q}_i^{(2)})), \quad (1)$$

where  $B$  denotes the batch size,  $q_i$  represents the ground-truth quality score (either a mean opinion score (MOS) for an original video or a pseudo-MOS for a generated variant), and  $\hat{q}_i$  is the predicted score. Superscripts (1) and (2) indicate the first and second video in the  $i$ -th pair, respectively.

Second, a direct quality score regression loss,  $\mathcal{L}_2$ , focuses on accurately predicting the absolute quality score for original videos:

$$\mathcal{L}_2 = \frac{\sum_{i=1}^B \mathbb{I}_{q_i^{(1)} \in \mathcal{M}} (q_i^{(1)} - \hat{q}_i^{(1)})^2}{\max(\sum_{i=1}^B \mathbb{I}_{q_i^{(1)} \in \mathcal{M}}, 1)}, \quad (2)$$

where  $\mathcal{M}$  is the set of ground-truth MOS values for original videos. The indicator function  $\mathbb{I}_{q_i^{(1)} \in \mathcal{M}}$  ensures  $\ell_2$  loss is calculated only for pairs where the first video is an original variant.

Third, an autoregressive text generation loss,  $\mathcal{L}_3$ , trains the model to produce relevant natural language descriptions of content and quality attributes:

$$\mathcal{L}_3 = -\frac{1}{\sum_{i=1}^B O_i} \sum_{i=1}^B \sum_{k=1}^{O_i} \log \hat{p}_{i,k}(z_{i,k}), \quad (3)$$

where  $O_i$  is the length of the target text sequence  $z_i$  for the  $i$ -th sample, and  $\hat{p}_{i,k}(z_{i,k})$  is the predicted probability of the  $k$ -th target token. This standard cross-entropy loss for next-token prediction is applied only to the generated token sequence representing the descriptive output. The total loss function  $\mathcal{L}$  is a weighted combination of these individual losses.

## 4 Experiments

### 4.1 Experimental Setups

**Datasets.** The proposed model, CP-LLM, was trained on LSVQ [32] and augmented with compression variants. These variants were generated by encoding the original LSVQ videos using the

Model	MOS SRCC/PLCC $\uparrow$	DMOS SRCC/PLCC $\uparrow$	FR $\downarrow$
FastVQA [25]	0.759 / 0.768	0.272 / 0.380	0.220
DOVER [26]	0.783 / 0.798	0.399 / 0.516	0.170
Q-Align [29]	<u>0.795 / 0.799</u>	<u>0.507 / 0.581</u>	<u>0.118</u>
CP-LLM (ours)	<b>0.801 / 0.800</b>	<b>0.540 / 0.605</b>	<b>0.085</b>

Table 1: MOS/DMOS correlations and flip rates evaluated on the YT-Compress dataset. The top-2 results are highlighted in **bold** and underline.

H.264 codec at 20 distinct constant rate factor (CRF) levels, ranging from 15 to 53. A foundational assumption in this process is that the perceptual quality of a variant encoded at a higher CRF level (*i.e.*, lower bitrate) does not exceed that of a variant encoded at a lower CRF level (*i.e.*, higher bitrate). To train the language decoder component of CP-LLM, videos from LSVQ were annotated using Gemini 2.0, prompted with: “*Based on the provided video frames, create a three-sentence summary. First, describe the visual content of the video in detail. Second, identify the style of the video. Third, assess the technical quality.*” These generated annotations constitute a crucial part of the training data for the language decoder. For evaluation, the performance of CP-LLM was assessed on five diverse UGC datasets selected for their varied content types and distortion characteristics: YT-Compress [19], YouTubeUGC [19], LIVE-YT-Gaming [36], Shorts-SDR [21], and Shorts-HDR2SDR [21].

**Evaluated VQA models.** We compare our proposed model against a representative set of SOTA VQA methods. This includes several prominent deep learning-based models: CoINVQ [20], FastVQA [25], and DOVER [26]. To benchmark with recent multimodal approaches, we also include the MLLM-based method Q-Align [29] and one commercial MLLM Gemini 2.0.

**Quality Predictor Performance Criteria.** The model performance is evaluated by three criteria: the Spearman’s rank correlation coefficient (SRCC) measures the prediction monotonicity, the Pearson linear correlation coefficient (PLCC) assesses the prediction linearity, the flip rate (FR) quantifies sensitivity to pixel-level alterations, measuring the percentage of incorrectly ranked pairs of videos derived from the same source but with different compression levels. Higher values for SRCC and PLCC, and lower values for FR indicate better performance.

**Implementation Details.** We set the number of key frames  $M = 5$  per video for LSVQ, Shorts-SDR and Shorts-HDR2SDR,  $M = 8$  for LIVE-YT-Gaming,  $M = 19$  for YT-Compress and YouTube-UGC. Key frames were processed via two pipelines: 1) bilinear resizing to  $448 \times 448$  pixels ignoring aspect ratio for the SigLIP [1] encoder, and 2) bilinear resizing preserving aspect ratio to fit within  $540 \times 1080$  pixels, followed by cropping  $K = 8$  non-overlapping  $224 \times 224$  pixel patches for the low-level vision encoder VideoPrism [39]. The maximum sequence length was set to  $L = 512$  tokens. We fine-tuned the Gemma [16] language decoder using low-rank adaptation (LoRA) [5], applying a rank of  $R = 4$  to its query, key, and value attention projections. This fine-tuning process utilized the same prompt that guided the initial data annotation phase. During this process, the high-level vision encoder remained fixed, while the entire low-level vision encoder and the quality regression head underwent full fine-tuning. Optimization was performed with the multi-task loss with equal weights using the Adam optimizer [6] for 500 epochs with a batch size of 128 and an initial learning rate of  $\eta = 1 \times 10^{-4}$  on a 16-core TPU v5.

## 4.2 Experiment Results

Table 1 compares the VQA model accuracy and robustness on the YT-Compress dataset, evaluating by SRCC/PLCC on mean opinion scores (MOS) and differential mean opinion scores (DMOS), and flip rate (FR) on pairs of compression variants. We can see CP-LLM achieves superior performance on all three dimensions. Specifically, it surpasses Q-Align, another MLLM-based approach. This suggests that CP-LLM not only excels in making accurate quality assessments for single videos but is also sensitive at detecting distortions within the same contents. Moreover, although trained exclusively with H.264 compression, the model demonstrates notable robustness to the VP9 compression present in the YT-Compress dataset.

The cross-dataset MOS correlations are shown in Table 2. These four datasets represent highly challenging and recent VQA benchmarks, with content that diverges substantially from the LSVQ

SRCC/PLCC↑	YouTube-UGC	LIVE-YT-Gaming	Shorts-SDR	Shorts-HDR2SDR
FastVQA [25]	0.730 / 0.747	0.619 / 0.666	<b>0.791</b> / 0.800	0.530 / 0.652
DOVER [26]	0.777 / 0.792	<b>0.668</b> / <b>0.726</b>	0.768 / 0.799	0.512 / 0.614
MBVQA [23]	0.788 / 0.804	0.600 / 0.696	0.753 / <u>0.802</u>	0.559 / <u>0.686</u>
Q-Align [29]	<b>0.833</b> / <b>0.846</b>	0.611 / 0.687	0.746 / 0.779	<u>0.585</u> / 0.672
CP-LLM (ours)	<u>0.810</u> / <u>0.813</u>	<u>0.620</u> / <u>0.702</u>	0.759 / <b>0.804</b>	<b>0.586</b> / <b>0.708</b>

Table 2: Cross-dataset testing of our model against four competing models, all retrained on the official training split of the large-scale LSVQ dataset and tested on other VQA datasets without fine-tuning. The top-2 results on each dataset are highlighted in **bold** and underline.

FR↓	Answer / Score	Diff=2	Diff=4	Diff=6	Diff=8	Diff=10	Diff=20
Gemini 2.0	Answer	0.502	0.434	0.385	0.348	0.319	0.181
CoINVQ [20]	Score	0.167	<u>0.142</u>	0.123	0.108	0.086	<u>0.006</u>
FastVQA [25]	Score	0.256	0.205	0.169	0.150	0.111	0.024
DOVER [26]	Score	0.268	0.218	0.179	0.156	0.126	0.026
Q-Align [29]	Score	<u>0.162</u>	<u>0.142</u>	<u>0.122</u>	<u>0.105</u>	<u>0.082</u>	0.008
CP-LLM (ours)	Score	<b>0.125</b>	<b>0.069</b>	<b>0.048</b>	<b>0.033</b>	<b>0.021</b>	<b>0.002</b>

Table 3: Flip rate test results for our proposed model versus five competing models, evaluated on LSVQ-test-1080p and its compression variants. “Answer / Score” denotes if the model’s comparison output is a textual answer or a numerical score; “Diff” indicates the CRF difference between compression pairs. The top-2 results are highlighted in **bold** and underline.

training set. CP-LLM achieves a top-2 ranking across these four datasets, demonstrating satisfactory generalization capabilities.

Table 3 shows the flip rate results observed across 20 distinct compression variants of the LSVQ-test-1080p dataset, aiming to evaluate the fine-grained distortion sensitivity. CP-LLM showcases superior sensitivity to pixel-level distortions, outperforming all other models. This highlights the efficacy of CP-LLM’s architecture and comprehensive training strategy in capturing pixel-level artifacts. Notably, prominent models such as Gemini 2.0, considered a leading MLLM, and DOVER, a SOTA VQA model, exhibit limitations in reliably distinguishing small pixel-level distortions. This suggests that in the absence of the proposed quality-related pairwise training, even highly capable models may struggle with such fine-grained perceptual distinctions.

In addition to the quantitative results presented above, qualitative examples are provided to further illustrate CP-LLM’s capabilities. Figure 5 demonstrates that when performing inference with a single input, CP-LLM can generate detailed descriptions of content and quality, accompanied by a predicted score. Figure 6 illustrates that during inference with pairwise inputs, CP-LLM is capable of determining which input exhibits superior quality and provides precise quality scores for each input.

### 4.3 Ablation Studies

We conduct a series of ablation studies to evaluate the impact of key design choices within our proposed model, specifically examining: 1) different input pipeline strategies (Tables 4a and 4b) and 2) various fine-tuning approaches for the high-level vision encoder (Tables 4c and 4d). Each ablated component is assessed based on its performance with MOS from the two of the LSVQ test sets, reported using SRCC/PLCC, and additionally on their compression variants, evaluated using FR.

Analysis of the input pipeline strategy indicates that a mixed approach, combining single-frame and pairwise inputs, yields superior SRCC/PLCC values compared to employing either mode in isolation. While a purely pairwise strategy is most effective for minimizing the FR, the mixed strategy provides a robust overall balance across these performance metrics. Regarding the high-level vision encoder, freezing all layers was found to optimize SRCC/PLCC performance while minimizing the number of trainable parameters and maintaining a competitive FR. Although fine-tuning all layers achieves the



SRCC/PLCC↑	LSVQ-test	LSVQ-1080p
Single	0.748 / 0.751	0.620 / 0.674
Pairwise	0.667 / 0.684	0.523 / 0.599
Mix	<b>0.851 / 0.850</b>	<b>0.747 / 0.796</b>

(a) **Input pipeline strategy (SRCC/PLCC).** A mixed input pipeline significantly outperforms strategies relying solely on single-frame or pairwise inputs in terms of SRCC and PLCC scores.

SRCC/PLCC↑	LSVQ-test	LSVQ-1080p
Frozen	<b>0.851 / 0.850</b>	<b>0.747 / 0.796</b>
Head	0.800 / 0.802	0.654 / 0.718
All	0.831 / 0.832	0.705 / 0.750

(c) **High-level vision encoder fine-tuning (SRCC/PLCC).** Freezing all layers of the SigLIP [1] high-level vision encoder yields optimal SRCC/PLCC scores with minimal trainable parameters compared to fine-tuning only the head or all layers.

FR↓	LSVQ-test	LSVQ-1080p
Single	0.217	0.259
Pairwise	<b>0.055</b>	<b>0.063</b>
Mix	0.072	0.082

(b) **Input pipeline strategy (Flip Rate).** The pairwise input strategy achieves the lowest flip rate, while the mixed strategy offers a better balance between SRCC/PLCC and FR.

FR↓	LSVQ-test	LSVQ-1080p
Frozen	0.072	0.082
Head	0.103	0.122
All	<b>0.055</b>	<b>0.054</b>

(d) **High-level vision encoder fine-tuning (Flip Rate).** While fine-tuning all SigLIP layers achieves the lowest flip rate, the default strategy of freezing all layers maintains a competitive flip rate with much lower training costs.

Table 4: Ablation experiments.

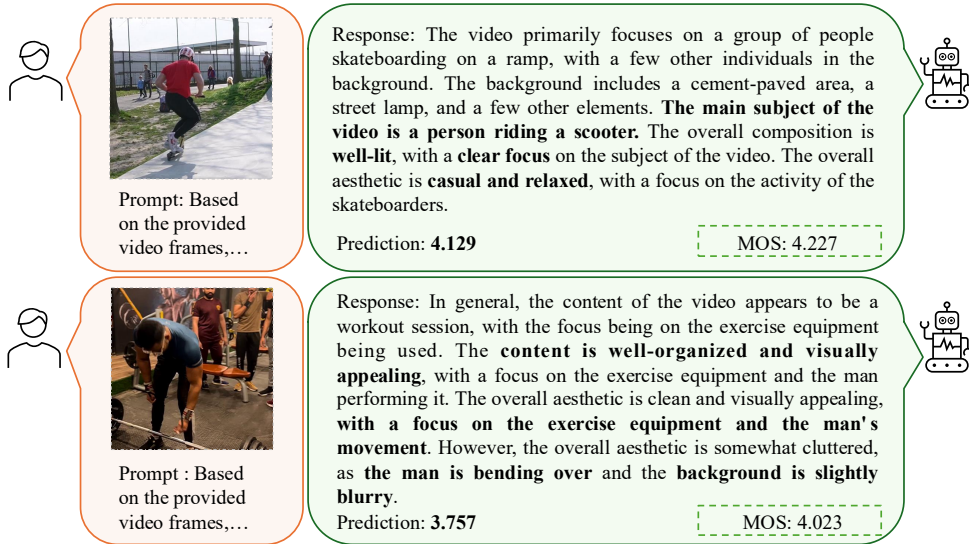


Figure 5: Single video quality score prediction and textual explanation by CP-LLM.

lowest absolute FR, freezing all layers still yields satisfactory results for this metric and offers a more favorable trade-off when all performance aspects are considered.

## 5 Conclusion and Discussion

We have presented CP-LLM, a novel MLLM-based framework for VQA that simultaneously predicts quality scores and generates interpretable textual descriptions. Our method addresses key challenges in VQA, particularly the perception of pixel-level distortions and the integration of quantitative and qualitative feedback, leveraging dual vision encoders and a multi-task training strategy. Comprehensive experiments and ablation studies verify the effectiveness of CP-LLM’s design in achieving robust video quality assessment. Additionally, the model’s dual-output architecture provides a comprehensive insight into video quality beyond a single score.



Figure 6: Pairwise video comparison results by CP-LLM, with zoom-in differences highlighted by the red box (not feed into the model).

The current work serves as an important step towards MLLM-based VQA, yet limitations for future research persist. For example, the language decoder currently imposes an input token limit, which restricts the number of video frames that can be processed simultaneously from very long sequences. Exploring more efficient video tokenization strategies to extend the effective input context length is a compelling direction for future work. Furthermore, future investigations could focus on MLLMs within active learning frameworks, potentially for generating sophisticated pseudo-label and boosting VQA model performance.

## References

- [1] Xi Chen, Xiao Wang, Lucas Beyer, Alexander Kolesnikov, Jialin Wu, Paul Voigtlaender, Basil Mustafa, Sebastian Goodman, Ibrahim Alabdulmohsin, Piotr Padlewski, Daniel Salz, Xi Xiong, Daniel Vlasic, Filip Pavetic, Keran Rong, Tianli Yu, Daniel Keysers, Xiaohua Zhai, and Radu Soricut. PaLi-3 vision language models: Smaller, faster, stronger. *arXiv preprint arXiv:2310.09199*, 2023.
- [2] Alexey Dosovitskiy, Lucas Beyer, Alexander Kolesnikov, Dirk Weissenborn, Xiaohua Zhai, Thomas Unterthiner, Mostafa Dehghani, Matthias Minderer, Georg Heigold, Sylvain Gelly, Jakob Uszkoreit, and Neil Houlsby. An image is worth 16x16 words: Transformers for image recognition at scale. In *International Conference on Learning Representations*, pages 1–22, 2021.
- [3] Christoph Feichtenhofer, Haoqi Fan, Jitendra Malik, and Kaiming He. SlowFast networks for video recognition. In *IEEE International Conference on Computer Vision*, pages 6202–6211, 2019.
- [4] Qihang Ge, Wei Sun, Yu Zhang, Yunhao Li, Zhongpeng Ji, Fengyu Sun, Shangling Jui, Xiongkuo Min, and Guangtao Zhai. LMM-VQA: Advancing video quality assessment with large multimodal models. *arXiv preprint arXiv:2408.14008*, 2024.
- [5] Edward J. Hu, Yelong Shen, Phillip Wallis, Zeyuan Allen-Zhu, Yanzhi Li, Shean Wang, Lu Wang, and Weizhu Chen. LoRA: Low-rank adaptation of large language models. In *International Conference on Learning Representations*, pages 1–16, 2022.
- [6] Diederik Kingma and Jimmy Ba. Adam: A method for stochastic optimization. In *International Conference on Learning Representations*, pages 1–15, 2015.
- [7] Jari Korhonen. Two-level approach for no-reference consumer video quality assessment. *IEEE Transactions on Image Processing*, 28(12):5923–5938, 2019.
- [8] Jari Korhonen, Yicheng Su, and Junyong You. Blind natural video quality prediction via statistical temporal features and deep spatial features. In *ACM International Conference on Multimedia*, pages 3311–3319, 2020.

- [9] Bowen Li, Weixia Zhang, Meng Tian, Guangtao Zhai, and Xianpei Wang. Blindly assess quality of in-the-wild videos via quality-aware pre-training and motion perception. *IEEE Transactions on Circuits and Systems for Video Technology*, 32(9):5944–5958, 2022.
- [10] Dingquan Li, Tingting Jiang, and Ming Jiang. Quality assessment of in-the-wild videos. In *ACM International Conference on Multimedia*, pages 2351–2359, 2019.
- [11] Zhi Li, Christos Bampis, Julie Novak, Anne Aaron, Kyle Swanson, Anush K. Moorthy, and J.D. Cock. VMAF: The journey continues. *Netflix Technology Blog*, 25(1), 2018.
- [12] Anish Mittal, Michele A. Saad, and Alan C. Bovik. A completely blind video integrity oracle. *IEEE Transactions on Image Processing*, 25(1):289–300, 2016.
- [13] Michele A. Saad, Alan C. Bovik, and Christophe Charrier. Blind prediction of natural video quality. *IEEE Transactions on Image Processing*, 23(3):1352–1365, 2014.
- [14] Wei Sun, Xiongkuo Min, Wei Lu, and Guangtao Zhai. A deep learning based no-reference quality assessment model for UGC videos. In *ACM International Conference on Multimedia*, pages 856–865, 2022.
- [15] Wei Sun, Wen Wen, Xiongkuo Min, Long Lan, Guangtao Zhai, and Kede Ma. Analysis of video quality datasets via design of minimalistic video quality models. *IEEE Transactions on Pattern Analysis and Machine Intelligence*, 46(11):7056–7071, 2024.
- [16] Gemma Team and Google DeepMind. Gemma: Open models based on gemini research and technology. *arXiv preprint arXiv:2403.08295*, 2024.
- [17] Zhengzhong Tu, Yilin Wang, Neil Birkbeck, Balu Adsumilli, and Alan C. Bovik. UGC-VQA: Benchmarking blind video quality assessment for user generated content. *IEEE Transactions on Image Processing*, 30:4449–4464, 2021.
- [18] Zhengzhong Tu, Xiangxu Yu, Yilin Wang, Neil Birkbeck, Balu Adsumilli, and Alan C. Bovik. RAPIQUE: Rapid and accurate video quality prediction of user generated content. *IEEE Open Journal of Signal Processing*, 2:425–440, 2021.
- [19] Yilin Wang, Sasi Inguva, and Balu Adsumilli. YouTube UGC dataset for video compression research. In *IEEE International Workshop on Multimedia Signal Processing*, pages 1–5, 2019.
- [20] Yilin Wang, Junjie Ke, Hossein Talebi, Joong Gon Yim, Neil Birkbeck, Balu Adsumilli, Peyman Milanfar, and Feng Yang. Rich features for perceptual quality assessment of UGC videos. In *IEEE Conference on Computer Vision and Pattern Recognition*, pages 13435–13444, 2021.
- [21] Yilin Wang, Joong Gon Yim, Neil Birkbeck, and Balu Adsumilli. YouTube SFV+ HDR quality dataset. In *IEEE International Conference on Image Processing*, pages 96–102. IEEE, 2024.
- [22] Zhou Wang, Alan C. Bovik, Hamid R. Sheikh, and Eero P. Simoncelli. Image quality assessment: From error visibility to structural similarity. *IEEE Transactions on Image Processing*, 13(4):600–612, 2004.
- [23] Wen Wen, Mu Li, Yabin Zhang, Yiting Liao, Junlin Li, Li Zhang, and Kede Ma. Modular blind video quality assessment. In *IEEE Conference on Computer Vision and Pattern Recognition*, pages 2763–2772, 2024.
- [24] Wen Wen, Yilin Wang, Neil Birkbeck, and Balu Adsumilli. An ensemble approach to short-form video quality assessment using multimodal llm. In *IEEE International Conference on Acoustics, Speech & Signal Processing*, pages 1–5, 2025.
- [25] Haoning Wu, Chaofeng Chen, Jingwen Hou, Liang Liao, Annan Wang, Wenxiu Sun, Qiong Yan, and Weisi Lin. FAST-VQA: Efficient end-to-end video quality assessment with fragment sampling. In *European Conference on Computer Vision*, pages 538–554, 2022.
- [26] Haoning Wu, Erli Zhang, Liang Liao, Chaofeng Chen, Jingwen Hou, Annan Wang, Wenxiu Sun, Qiong Yan, and Weisi Lin. Exploring video quality assessment on user generated contents from aesthetic and technical perspectives. In *IEEE International Conference on Computer Vision*, pages 20144–20154, 2023.

- [27] Haoning Wu, Zicheng Zhang, Erli Zhang, Chaofeng Chen, Liang Liao, Annan Wang, Chunyi Li, Wenxiu Sun, Qiong Yan, Guangtao Zhai, and Weisi Lin. Q-Bench: A benchmark for general-purpose foundation models on low-level vision. In *International Conference on Learning Representations*, pages 1–13, 2024.
- [28] Haoning Wu, Zicheng Zhang, Erli Zhang, Chaofeng Chen, Liang Liao, Annan Wang, Kaixin Xu, Chunyi Li, Jingwen Hou, Guangtao Zhai, Geng Xue, Wenxiu Sun, Qiong Yan, and Weisi Lin. Q-Instruct: Improving low-level visual abilities for multi-modality foundation models. In *IEEE Conference on Computer Vision and Pattern Recognition*, pages 25490–25500, 2024.
- [29] Haoning Wu, Zicheng Zhang, Weixia Zhang, Chaofeng Chen, Liang Liao, Chunyi Li, Yixuan Gao, Annan Wang, Erli Zhang, Wenxiu Sun, Qiong Yan, Xiongkuo Min, Guangtao Zhai, and Weisi Lin. Q-Align: Teaching LMMs for visual scoring via discrete text-defined levels. In *International Conference on Machine Learning*, pages 81–92, 2024.
- [30] Haoning Wu, Hanwei Zhu, Zicheng Zhang, Erli Zhang, Chaofeng Chen, Liang Liao, Chunyi Li, Annan Wang, Wenxiu Sun, Qiong Yan, Xiaohong Liu, Guangtao Zhai, Shiqi Wang, and Weisi Lin. Towards open-ended visual quality comparison. In *European Conference on Computer Vision*, pages 360–377. Springer, 2024.
- [31] Tianhe Wu, Kede Ma, Jie Liang, Yujiu Yang, and Lei Zhang. A comprehensive study of multimodal large language models for image quality assessment. In *European Conference on Computer Vision*, pages 143–160. Springer, 2024.
- [32] Zhenqiang Ying, Maniratnam Mandal, Deepti Ghadiyaram, and Alan C. Bovik. Patch-VQ: ‘Patching up’ the video quality problem. In *IEEE Conference on Computer Vision and Pattern Recognition*, pages 14019–14029, 2021.
- [33] Zhiyuan You, Xin Cai, Jinjin Gu, Tianfan Xue, and Chao Dong. Teaching large language models to regress accurate image quality scores using score distribution. In *IEEE Conference on Computer Vision and Pattern Recognition*, to appear, 2025.
- [34] Zhiyuan You, Jinjin Gu, Zheyuan Li, Xin Cai, Kaiwen Zhu, Chao Dong, and Tianfan Xue. Descriptive image quality assessment in the wild. *arXiv preprint arXiv:2405.18842*, 2024.
- [35] Zhiyuan You, Zheyuan Li, Jinjin Gu, Zhenfei Yin, Tianfan Xue, and Chao Dong. Depicting beyond scores: Advancing image quality assessment through multi-modal language models. In *European Conference on Computer Vision*, pages 259–276. Springer, 2024.
- [36] Xiangxu Yu, Zhengzhong Tu, Zhenqiang Ying, Alan C. Bovik, Neil Birkbeck, Yilin Wang, and Balu Adsumilli. Subjective quality assessment of user-generated content gaming videos. In *IEEE Winter Conference on Applications of Computer Vision*, pages 74–83, 2022.
- [37] Richard Zhang, Phillip Isola, Alexei A. Efros, Eli Shechtman, and Oliver Wang. The unreasonable effectiveness of deep features as a perceptual metric. In *IEEE Conference on Computer Vision and Pattern Recognition*, pages 586–595, 2018.
- [38] Zicheng Zhang, Ziheng Jia, Haoning Wu, Chunyi Li, Zijian Chen, Yingjie Zhou, Wei Sun, Xiaohong Liu, Xiongkuo Min, Weisi Lin, and Guangtao Zhai. Q-Bench-Video: Benchmarking the video quality understanding of LMMs. In *IEEE Conference on Computer Vision and Pattern Recognition*, to appear, 2025.
- [39] Long Zhao, Nitesh Bharadwaj Gundavarapu, Liangzhe Yuan, Hao Zhou, Shen Yan, Jennifer J Sun, Luke Friedman, Rui Qian, Tobias Weyand, Yue Zhao, Rachel Hornung, Florian Schroff, Ming-Hsuan Yang, David A. Ross, Huisheng Wang, Hartwig Adam, Mikhail Sirotenko, Ting Liu, and Boqing Gong. VideoPrism: A foundational visual encoder for video understanding. In *International Conference on Machine Learning*, pages 60785–60811. PMLR, 2024.